Mon. Not. R. Astron. Soc. **370,** 1752–1762 (2006) doi:10.1111/j.1365-2966.2006.10587.x

SN 2005cs in M51 – I. The first month of evolution of a subluminous SN II plateau

A. Pastorello,[1⋆] D. Sauer,[2] S. Taubenberger,[1] P. A. Mazzali[1,2,3,4] K. Nomoto,[3,4] K. S. Kawabata,[5] S. Benetti,[6] N. Elias-Rosa,[6] A. Harutyunyan,[6] H. Navasardyan,[6] L. Zampieri,[6] T. Iijima,[7] M. T. Botticella,[8,9] G. Di Rico,[8,9] M. Del Principe,[9] M. Dolci,[9] S. Gagliardi,[9] M. Ragni[8,9] and G. Valentini[9]

[1]*Max-Planck-Institut für Astrophysik, Karl-Schwarzschild-Str. 1, 85741 Garching bei München, Germany*
[2]*INAF Osservatorio Astronomico di Trieste, Via Tiepolo 11, 34131 Trieste, Italy*
[3]*Department of Astronomy, School of Science, University of Tokyo, Bunkyo-ku, Tokyo 113-0033, Japan*
[4]*Research Center for the Early Universe, School of Science, University of Tokyo, Bunkyo-ku, Tokyo 113-0033, Japan*
[5]*Hiroshima Astrophysical Science Center, Hiroshima University, Hiroshima 739-8526, Japan*
[6]*INAF Osservatorio Astronomico di Padova, Vicolo dell'Osservatorio 5, 35122 Padova, Italy*
[7]*INAF Osservatorio Astronomico di Padova, Sezione di Asiago, Via dell'Osservatorio 8, 36012 Asiago (Vicenza), Italy*
[8]*Università degli Studi di Teramo, Viale Crucioli 122, 64100 Teramo, Italy*
[9]*INAF Osservatorio Astronomico di Collurania, via M. Maggini, 64100 Teramo, Italy*

Accepted 2006 May 18. Received 2006 May 18; in original form 2005 November 7

ABSTRACT

Early-time optical observations of supernova (SN) 2005cs in the Whirlpool Galaxy (M51) are reported. Photometric data suggest that SN 2005cs is a moderately underluminous Type II plateau SN (SN IIP). The SN was unusually blue at early epochs ($U - B \approx -0.9$ about three days after explosion) which indicates very high continuum temperatures. The spectra show relatively narrow P Cygni features, suggesting ejecta velocities lower than observed in more typical SNe IIP. The earliest spectra show weak absorption features in the blue wing of the He I 5876-Å absorption component and, less clearly, of Hβ and Hα. Based on spectral modelling, two different interpretations can be proposed: these features may either be due to high-velocity H and He I components, or (more likely) be produced by different ions (N II, Si II). Analogies with the low-luminosity, ^{56}Ni-poor, low-velocity SNe IIP are also discussed. While a more extended spectral coverage is necessary in order to determine accurately the properties of the progenitor star, published estimates of the progenitor mass seem not to be consistent with stellar evolution models.

Key words: supernovae: general – supernovae: individual: SN 2005cs – supernovae: individual: SN 1997D – supernovae: individual: SN 1999br – supernovae: individual: SN 2003Z – galaxies: individual: M51.

1 INTRODUCTION

Type II supernovae (SNe II) are believed to be produced by the explosion following the core-collapse of massive stars that retained most of their H envelope at the time of explosion. Some SNe II spend a period at almost constant luminosity: this phase, lasting sometimes a few months, is called 'plateau' (hence the label SN IIP). When the SN enters this phase, the temperature is low enough that the massive H envelope, initially ionized because of the deposition of energy by the shock wave, starts to recombine. After recombination, the light curve of SNe IIP declines steeply, until it settles on to the 'radioactive tail', as do other SN Types. In this phase, the luminosity is due mainly to the radioactive decay of ^{56}Ni to ^{56}Co to ^{56}Fe.

Despite the considerable number of SNe IIP studied in recent years (e.g. Patat et al. 1994; Hamuy 2003), the physical properties of the progenitor stars are still a matter of debate. Thanks to the direct identification of several SN precursors in deep pre-explosion images, important constraints have been established on the nature of the progenitors of SNe IIP. The first SN with a known progenitor was SN 1987A in the Large Magellanic Cloud. Archival images showed that the supergiant progenitor was unusually blue (e.g. Sonneborn, Altner & Kirshner 1987). The present ensemble of SNe IIP with detected progenitor includes SN 2003gd (Van Dyk, Li & Filippenko

⋆E-mail: pasto@MPA-Garching.MPG.DE

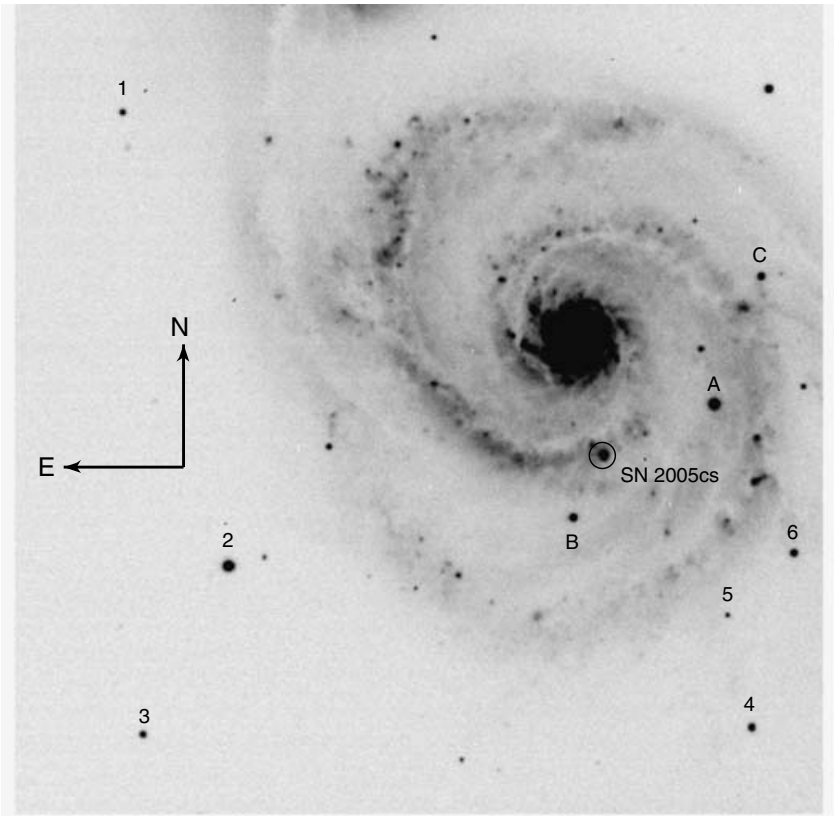

Figure 1. SN 2005cs in M51: *V*-band image obtained on 2005 July 1 with the Copernico 1.82-m telescope of Mt. Ekar, Asiago (Italy). The sequence stars from Richmond et al. (1996) are labelled with letters. Some of our local sequence standards (Pastorello et al., in preparation) are indicated by numbers.

2003; Hendry et al. 2005; Smartt et al. 2004), SN 2004et (Li et al. 2005), SN 1999ev (Maund & Smartt 2005) and, now, SN 2005cs (Maund, Smartt & Danziger 2005; Li et al. 2006). Lower magnitude limits or ambiguous detections have been obtained for other SNe IIP precursors (e.g. SN 1999br; Maund & Smartt 2005). All these observations seem to support the idea that most SNe IIP originate from the explosion of moderately massive stars ($M \leqslant 15_{\odot}$).

SN 2005cs was discovered in the famous Whirlpool Galaxy (NGC 5194 or M51) by Kloehr et al. (2005) on 2005 June 28.905 UT. Modjaz et al. (2005) classified it as a young Type II SN. The earliest detection was that of M. Fiedler on June 27.91 UT (SNWeb[1]). Nothing was visible on June 20.6 UT (Kloehr et al. 2005) at the SN position. Moreover, no clear detection of SN 2005cs was found on several different images obtained on June 26 by other amateur observers (SNWeb). In particular, the SN site was monitored by the team of the Osservatorio Astronomico 'Geminiano Montanari' (Cavezzo, Modena, Italy) on June 26.89 using a Newton 0.4-m telescope and nothing was detected below the following limits: $B \geqslant 17.3$, $V \geqslant 17.7$, $R \geqslant 17.6$. These detection limits constrain the explosion time to a very small uncertainty (about 1 d). Therefore, in this paper we adopt June 27.5 UT (JD = 245 3549 ± 1) as the explosion epoch.

The coordinates of SN 2005cs are $\alpha = 13^{\rm h}29^{\rm m}52\overset{\rm s}{.}85$ and $\delta = +47^{\circ}10'36\overset{''}{.}3$ (J2000). The object lies in the southern arm of M51, 15-arcsec west and 67.3-arcsec south of the galaxy nucleus (Fig. 1). M51 is classified by NASA/IPAC Extragalactic Database (NED)[2] as a SA(s)bc peculiar galaxy. The galaxy also hosted the well-studied core-collapse SN 1994I (Wheeler et al. 1994; Filippenko et al. 1995; Clocchiatti et al. 1996; Richmond et al. 1996).

A candidate progenitor for SN 2005cs was identified in combined *Hubble Space Telescope* (*HST*) ACS F814W images ($\sim I$ band) as a red supergiant ($M_{\rm ZAMS} = 9^{+3}_{-2}\,{\rm M}_{\odot}$) of spectral type in the range K0–M4 (Maund et al. 2005; Li et al. 2006). These two papers report different values for the *I*-band detection magnitude: 24.15 (i.e. absolute magnitude $M_I \approx -5.5$) and 23.3 ($M_I \approx -6.4$, adopting the same reddening and distance as Li et al. 2006), respectively. The position of the candidate as measured by Li et al. (2006) is $\alpha = 13^{\rm h}29^{\rm m}52\overset{\rm s}{.}76$, $\delta = +47^{\circ}10'36\overset{''}{.}11$ (J2000). Alternatively, Richmond (2005) claim that SN 2005cs exploded near a cluster of young stars and find that the progenitor candidate could be a blue star at $\alpha = 13^{\rm h}29^{\rm m}52\overset{\rm s}{.}803$, $\delta = +47^{\circ}10'36\overset{''}{.}52$ (J2000), with $M_V \approx -6$. However, since SN 2005cs is evolving like a normal plateau event (see Section 2), this blue supergiant progenitor candidate is not convincing.

Here, we present early-time optical observations of SN 2005cs (until ∼1 month after the explosion). In Section 2, we describe the photometric evolution of SN 2005cs and in Section 3 we analyse the spectroscopic data. A discussion follows in Section 4.

2 PHOTOMETRY

Our photometric data were obtained using seven different telescopes, and cover 19 epochs (including the pre-discovery limit), until approximately 35 d after the explosion.

[1]http://www.astrosurf.com/snweb2/
[2]http://nedwww.ipac.caltech.edu/

Table 1. *UBVRI* magnitudes of SN 2005cs and assigned errors. Both measurement errors and uncertainties in the photometric calibration (the most important source of errors) are taken into account. Measurement uncertainties give a minor contribution to the total error because, despite the relatively complex background, the SN was much brighter than any other nearby source.

Date (yy/mm/dd)	JD (+240 0000)	*U*	*B*	*V*	*R*	*I*	Inst.[a]
05/06/26	53548.39		$\geqslant$17.3	$\geqslant$17.7	$\geqslant$17.6		NCO
05/06/30	53552.36	13.48 ± 0.05	14.36 ± 0.05	14.48 ± 0.02	14.46 ± 0.04	14.44 ± 0.04	Caha
05/07/01	53553.35	13.53 ± 0.06	14.36 ± 0.05	14.46 ± 0.05	14.40 ± 0.02	14.34 ± 0.06	Ekar
05/07/02	53554.46	13.69 ± 0.10	14.45 ± 0.04	14.51 ± 0.03	14.47 ± 0.03	14.29 ± 0.10	Ekar
05/07/05	53557.42		14.52 ± 0.04	14.54 ± 0.04	14.42 ± 0.05	14.29 ± 0.08	Ekar
05/07/06	53557.84	14.02 ± 0.06	14.60 ± 0.05	14.55 ± 0.03	14.36 ± 0.03	14.40 ± 0.03	Sub
05/07/07	53559.40		14.65 ± 0.04	14.56 ± 0.09	14.41 ± 0.09	14.35 ± 0.11	TNT
05/07/11	53563.38	14.81 ± 0.05	14.87 ± 0.04	14.56 ± 0.04	14.37 ± 0.02	14.23 ± 0.05	Ekar
05/07/11	53563.42	14.89 ± 0.04	14.93 ± 0.04	14.53 ± 0.04	14.37 ± 0.03	14.26 ± 0.03	TNG
05/07/13	53565.38	15.27 ± 0.06	15.04 ± 0.05	14.64 ± 0.02	14.37 ± 0.03	14.29 ± 0.05	LT
05/07/14	53566.36	15.29 ± 0.05	15.11 ± 0.05	14.68 ± 0.02	14.44 ± 0.04	14.23 ± 0.02	Ekar
05/07/14	53566.40		15.09 ± 0.04	14.66 ± 0.04	14.40 ± 0.05	14.32 ± 0.06	TNT
05/07/17	53569.42	15.92 ± 0.07	15.31 ± 0.05	14.67 ± 0.03	14.40 ± 0.03	14.27 ± 0.04	LT
05/07/19	53571.40		15.36 ± 0.12	14.72 ± 0.05	14.45 ± 0.09	14.26 ± 0.07	TNT
05/07/20	53572.40		15.39 ± 0.07	14.71 ± 0.03	14.45 ± 0.03	14.27 ± 0.03	TNT
05/07/25	53577.40		15.46 ± 0.09	14.72 ± 0.04	14.36 ± 0.06	14.24 ± 0.06	TNT
05/07/27	53579.40		15.60 ± 0.07	14.73 ± 0.04	14.39 ± 0.04	14.16 ± 0.04	TNT
05/07/31	53583.39	16.83 ± 0.09	15.78 ± 0.06	14.71 ± 0.03	14.38 ± 0.03	14.12 ± 0.05	TNG
05/07/31	53583.47	16.81 ± 0.11	15.77 ± 0.06	14.69 ± 0.03	14.36 ± 0.03	14.15 ± 0.04	LT

[a]NCO – Osservatorio Cavezzo 40-cm Newton Telescope; Caha – Calar Alto 2.2-m Telescope + CAFOS; Ekar – Asiago 1.82-m Copernico Telescope + AFOSC; Sub – Subaru Telescope 8.2 m + FOCAS; TNG – Telescopio Nazionale Galileo 3.58 m + Dolores; LT – Liverpool Telescope 2.0 m + RATCAM; TNT – Teramo Normale Telescope 72 cm.

All data were pre-reduced with standard IRAF[3] procedures, and instrumental SN magnitudes were determined using the point spread function (PSF) fitting technique performed with the 'SNOOPY'[4] package. Since SN 2005cs is a bright object, this technique provides acceptable results, although the background region of SN 2005cs is extremely complicated, such that the subtraction of the template could be more appropriate when the SN fades.

In order to transform instrumental magnitudes to the standard Johnson–Cousins system, first-order colour corrections were applied with colour terms derived from observations of photometric standard fields (Landolt 1992). The photometric zero-points were finally determined by comparing the magnitudes of a local sequence of stars in the vicinity of M51 (cf. Fig. 1) to the values reported for some of these stars by Richmond et al. (1996) in their study on SN 1994I. A complete definitive photometry (calibrated on a larger sequence of stars, i.e. those labelled by numbers in Fig. 1) will be presented in a forthcoming paper (Pastorello et al., in preparation).

The SN magnitudes are reported in Table 1, and the *U*, *B*, *V*, *R* and *I* light curves are shown in Fig. 2 together with the light curves of SNe 1999br (Hamuy 2001; Pastorello et al. 2004) and 1999em (Hamuy et al. 2001; Leonard et al. 2002; Elmhamdi et al. 2003) shifted arbitrarily in magnitudes (but not in phase) in order to match the light curves of SN 2005cs. The overlap of the *B*-, *V*-, *R*- and *I*-band light curves of the three SNe is very good, while some differences are visible in the *U*-band evolution: the *U*-band light curve of SN 2005cs declines more rapidly than that of SN 1999em.

[3]IRAF is distributed by the National Optical Astronomy Observatories, which are operated by the Association of Universities for Research in Astronomy, Inc., under contract to the National Science Foundation.

[4]SNOOPY is a package implemented in IRAF by E. Cappellaro, based on DAOPHOT.

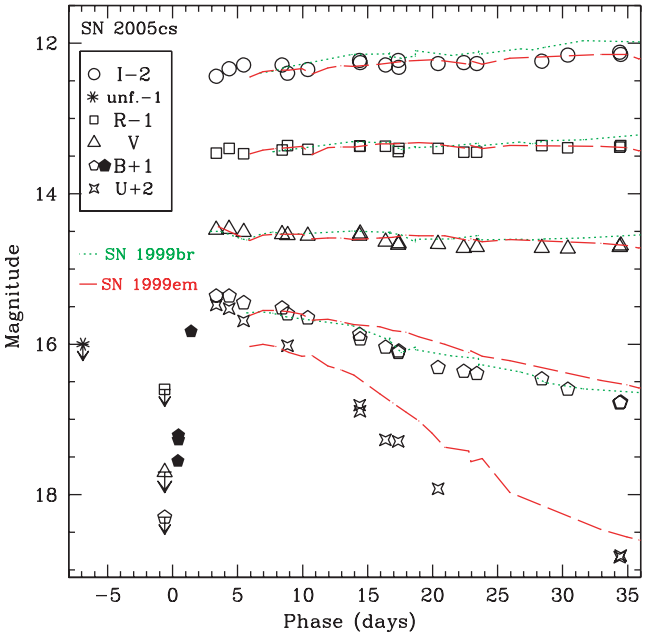

Figure 2. Early *U*, *B*, *V*, *R*, *I* light curves of SN 2005cs, including our limits of June 26 (when the SN was not detected) and the unfiltered limit from IAU Circ. 8853 (asterisk). Also, the light curves of SN 1999br (*BVRI*) and SN 1999em (*UBVRI*) have been included for comparison, and shifted in magnitude by an arbitrary amount in order to match the corresponding curves of SN 2005cs. The very early *B*-band detections of M. Fiedler (SNWeb) have been also reported (filled pentagons).

According to Modjaz et al. (2005), the simultaneous presence in the SN spectrum of narrow Galactic and host galaxy interstellar Na ID lines with analogous equivalent width (0.2 Å) indicates a similar contribution of the two components to the total extinction.

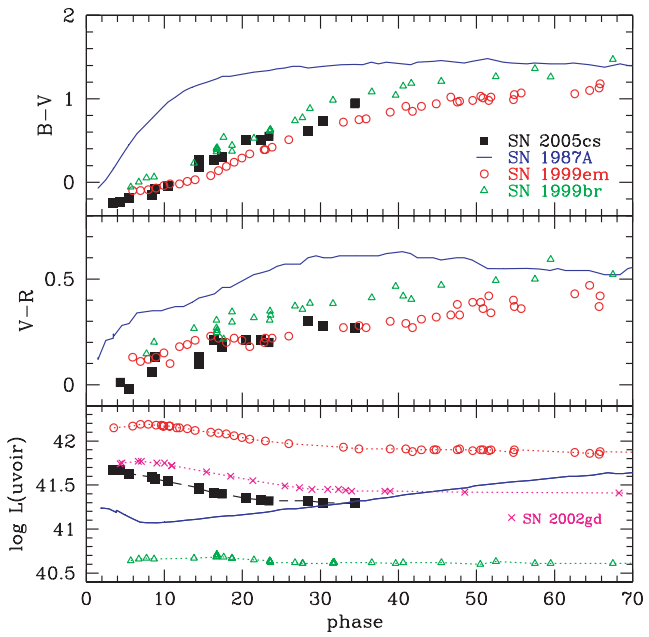

Figure 3. Top panel: early $B-V$ colour curve of SN 2005cs and those of SNe 1999em, 1999br and 1987A. Middle panel: same as above, but for $V-R$ colour. Bottom panel: early *uvoir* pseudo-bolometric light curves for the same sample of SNe IIP and, in addition, SN 2002gd. For references, see the text.

The host galaxy extinction can be estimated using the relation of Turatto, Benetti & Cappellaro (2003), while the value provided by Schlegel et al. (1998) is adopted for the Galactic extinction. Taking into account both components, a total reddening of $E(B-V)=0.06$ is estimated. However, other methods yield slightly higher values for the reddening. The study of the nearby H II region CCM 56 and the three-colour photometry of some red supergiants close to the SN position yield a total reddening of $E(B-V)=0.16$ (Bresolin, Gamett & Kennicutt 2004) and $E(B-V)=0.12$ (Maund et al. 2005), respectively. Lacking strong constraints in favour of one of these three methods, an average value of $E(B-V)=0.11\pm0.04$ is adopted. However, this relatively low amount of interstellar reddening is consistent with the blue colour of the early spectra of SN 2005cs.

Feldmeier, Ciardullo & Jacoby (1997) used planetary nebulae to determine a distance to M51 of 8.4 Mpc (i.e. distance modulus $\mu=29.62\pm0.15$). Averaging all R-band data reported in Table 1, an R-band absolute magnitude during the plateau phase $M_R\approx-15.48\pm0.16$ was obtained. This implies that SN 2005cs was relatively underluminous compared to more typical SNe IIP and was therefore similar to SNe 1997D and 1999br (Turatto et al. 1998; Benetti et al. 2001; Hamuy 2001; Zampieri et al. 2003; Pastorello et al. 2004), although less extreme.

In Fig. 3, we compare the early-time $B-V$ (top panel) and $V-R$ (middle panel) colour curves and the pseudo-bolometric *uvoir* light curve (bottom panel) of SN 2005cs with those of the SNe IIP 1999br (Hamuy 2001; Pastorello et al. 2004), 1999em (Hamuy et al. 2001; Leonard et al. 2002; Elmhamdi et al. 2003) and the peculiar 1987A (Menzies et al. 1987). The light curve of another moderately underluminous object, SN 2002gd (Pastorello 2003), is also included in Fig. 3 (bottom panel) for comparison.

We adopted a distance modulus $\mu=30.97$ and a total B-band extinction $A_B=0.10$ (Pastorello et al. 2004) for SN 1999br, $\mu=30.34$ (Leonard et al. 2003) and $A_B=0.41$ (Baron et al. 2000) for SN 1999em, $\mu=18.49$ and $A_B=0.79$ (Arnett et al. 1989) for SN 1987A, and $\mu=32.87$ and $A_B=0.29$ (Pastorello 2003) for SN 2002gd. Distance moduli for SNe 1999br and 2002gd were estimated from the recession velocity corrected for the Local Group infall on to the Virgo Cluster ($v_{\rm Vir}$), adopting a value of $H_0=72$ km s^{-1} Mpc^{-1}.

All typical SNe IIP show a similar colour evolution. Their colour curves become monotonically redder with time. On the other hand, SN 1987A was significantly redder at early epochs (until ∼50 d), but then the colour difference between it and other SNe IIP decreases with time. SN 2005cs follows the behaviour of SNe IIP: the $B-V$ colour increases from −0.2 to 1 during the first month, while the $V-R$ colour increases much more slowly (0–0.3) over the same period (Fig. 3, top and middle panels).

Interestingly, the *uvoir* light curve of SN 2005cs has an evolution reminiscent of that of normal SNe IIP (Fig. 3, bottom panel). The *uvoir* luminosity of SN 2005cs is intermediate between those of the intermediate ^{56}Ni mass SN 1999em ($M_{\rm Ni}\approx0.05\,{\rm M}_\odot$; Leonard et al. 2003) and the low-luminosity, ^{56}Ni-poor SN 1999br ($M_{\rm Ni}\approx2\times10^{-3}\,{\rm M}_\odot$; Zampieri et al. 2003; Pastorello et al. 2004), and is similar to that of the ^{56}Ni-poor SN 2002gd (see Section 4 and Pastorello 2003).

3 SPECTROSCOPY

Spectroscopy is available for 10 different epochs, ranging from about 3 to 35 d after the explosion. A summary of all spectroscopic observations is given in Table 2.

All raw frames were first bias and flat-field corrected, and then the SN spectra were optimally extracted. Wavelength calibration was obtained with the help of comparison lamp exposures, while the spectra were flux calibrated using standard star spectra obtained on the same night as the SN observations. When no spectrophotometric standard star was observed, a sensitivity function derived on a different night (close in time) was used. Telluric features were removed from the SN spectra, again using spectrophotometric standard spectra. However, the strong telluric band at 7570–7750 Å is superimposed on the O I λ7774 SN feature, and imperfect removal might significantly affect the profile of this line. Finally, all spectra were checked against the quasi-contemporaneous photometry and, where discrepancies occurred (especially during low-transparency or bad-seeing nights), the photometric data were used to derive a scaling factor to apply to the SN spectrum. The relative, final flux calibration was reasonable, and the agreement with photometry within 10 per cent.

3.1 Spectral evolution

We monitored SN 2005cs spectroscopically for about one month. There are only two significant observational gaps, between July 6 and 11 (phase 9–14 d) and between July 19 and 31 (phase 22–34 d). During the last part of the coverage, the spectrum of SN 2005cs evolved significantly. The spectral sequence is shown in Fig. 4.

The first spectra (phase 3–5 d) are characterized by a very blue continuum. The most prominent features are the P Cygni profiles of the H Balmer lines and He I 5876 Å. The position of the minimum of these lines indicates expansion velocities of the ejecta between 5000 and 8000 km s^{-1}, significantly lower than those typically observed in SNe IIP at a comparable phase (cf. e.g. Hamuy 2001, 2003; Pastorello 2003). The most intriguing property is the presence of absorption features on the blue side of Hβ, He I 5876 Å

Table 2. Journal of spectroscopic observations of SN 2005cs. The phase is from the explosion epoch.

Date (yy/mm/dd)	JD (+240 0000)	Phase (d)	Instrumental configuration[a]	Range (Å)	Resolution[b] (Å)
05/06/30	53552.44	3	CA3.5 m+PMAS+grt.V300	4700–8000	9
05/07/01	53553.41	4	Ekar+AFOSC+gm.4,2	3500–9200	24, 38
05/07/02	53554.39	5	Ekar+AFOSC+gm.4,2	3500–9200	24, 38
05/07/02	53554.45	5	Pennar+B&C+150tr/mm	4100–8700	25
05/07/05	53557.43	8	Ekar+AFOSC+gm.4,2	3650–9200	24, 38
05/07/06	53557.84	9	Subaru+FOCAS+B300+Y47	4800–9000	11
05/07/11	53563.36	14	Ekar+AFOSC+gm.4	3500–7800	24
05/07/11	53563.44	14	TNG+DOLORES+gm.LRB,LRR	3150–9500	18, 17
05/07/14	53566.35	17	Ekar+AFOSC+gm.4,2	3500–9200	24,38
05/07/15	53567.42	18	Pennar+B&C+150tr/mm	4150–8750	25
05/07/19	53571.45	22	Pennar+B&C+150tr/mm	4050–7900	25
05/07/31	53583.44	34	TNG+DOLORES+gm.LRB,LRR	3150–9600	18, 17

[a]CA3.5 m – 3.5-m Telescope, Calar Alto Obs., Centro Astr. Hispano Alemán, Almería (Spain); Ekar – 1.82-m Copernico Telescope, INAF – Osservatorio di Asiago, Mt. Ekar, Asiago (Italy); Pennar – 1.22-m Galilei Telescope, Università di Padova, Loc. Pennar, Asiago (Italy); Subaru – 8.2-m Subaru Telescope, National Astr. Obs. of Japan, Mauna Kea, Hawaii (USA); TNG – 3.5-m Telescopio Nazionale Galileo, La Palma, Canary Isl. (Spain).
[b]As measured from the full width at half-maximum (FWHM) of the night-sky lines.

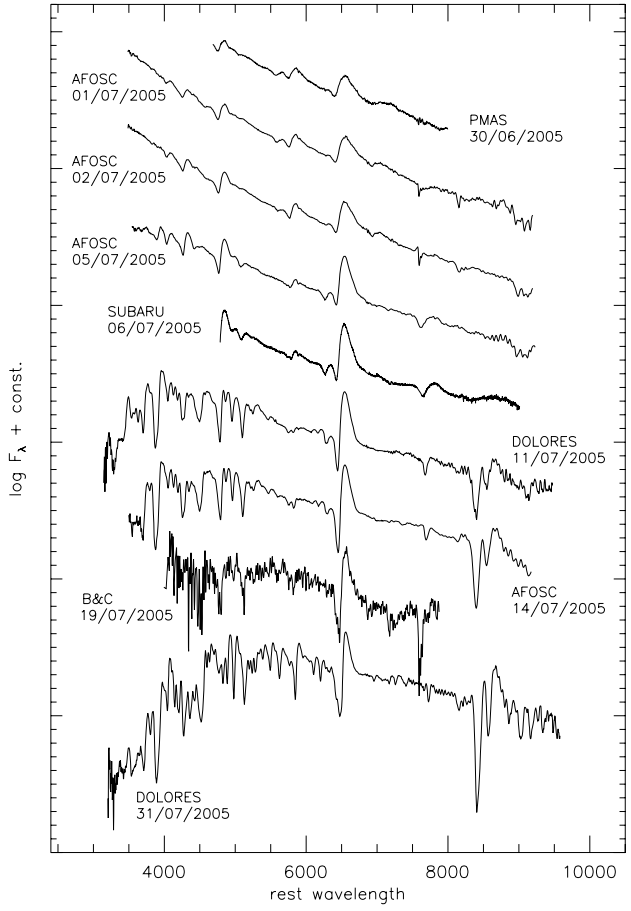

Figure 4. Spectroscopic evolution of SN 2005cs from ∼3 d to about one month after explosion. Telluric features were not removed from the noisy B& C spectrum of July 19. For details, see also Table 2. All spectra are at the host galaxy rest frame.

(very prominent) and, though this is clearly visible only in more evolved spectra, Hα. These absorptions can be interpreted as either high-velocity (HV) H I and He I features, or absorption lines of other ions (N II and Si II). The possible presence of HV lines could be explained either by an unusual density structure of the progenitor star, with a relatively dense and He-rich outer shell, or by strong mixing and asphericity of the ejecta. As discussed in Section 3.2, there is evidence that these lines are due to N II and Si II.

The subsequent two spectra (phase 8–9 d) also show a blue continuum, but the features near 4580 and 5580 Å have completely disappeared. The Fe II multiplet 42 lines ($\lambda\lambda$4924, 5018, 5169) begin to be visible to the red side of Hβ. The He I 5876-Å line becomes dimmer and a strong O I λ7774 line is now visible. Moreover, a very prominent absorption feature is now well developed at ∼6300 Å, close to the blue wing of the Hα absorption. We tentatively identify this line as the Si II 6347-, 6371-Å doublet (the feature that is prominent in the photospheric spectra of SNe Ia, hereafter Si II 6355 Å), rather than as a HV Hα component (see also Sections 3.2 and 3.3).

The spectra at phase 14–22 d show redder continua and lines with deeper P Cygni profiles. In the region below ∼5300 Å, together with the Balmer H lines, we identify several metal lines. In addition to strong lines of Fe II, Ti II and Sc II (e.g. the absorptions at 5250 and 5470 Å), Sr II $\lambda\lambda$4078, 4216 (doublet 1) and $\lambda\lambda$4162, 4305 (doublet 3) are possibly detected. Consistently with the lower effective temperature, the He I line is no longer visible and the feature near 5800 Å is probably due to the increasing strength of Na ID. Finally, Ca II H& K and the Ca II IR (infrared) triplet are now among the most prominent features. The components of the Ca II IR triplet are not blended, confirming the low ejecta velocity.

By the times of the last TNG (Telescopio Nazionale Galileo) observation, obtained about 34 d after the explosion, the spectrum has noticeably changed. Overall, it looks like a spectrum of a typical SN II during the recombination phase. The continuum is much redder, and the flux deficit below ∼3800 Å is due to strong line blanketing from the Fe II features (Mazzali, Lucy & Butler 1992), but other metal ions may also contribute significantly to the continuum shape. The most prominent lines are now Hα, Ca II H& K and the Ca II IR triplet, all with very well developed P Cygni profiles. A detailed line identification of this spectrum is presented in Section 3.3.

3.2 High-velocity H I, He I features or N II, Si II lines?

Fig. 5 shows the early evolution of the spectral region between 4100 and 7300 Å. The Hβ, He I 5876-Å and Hα absorption minima

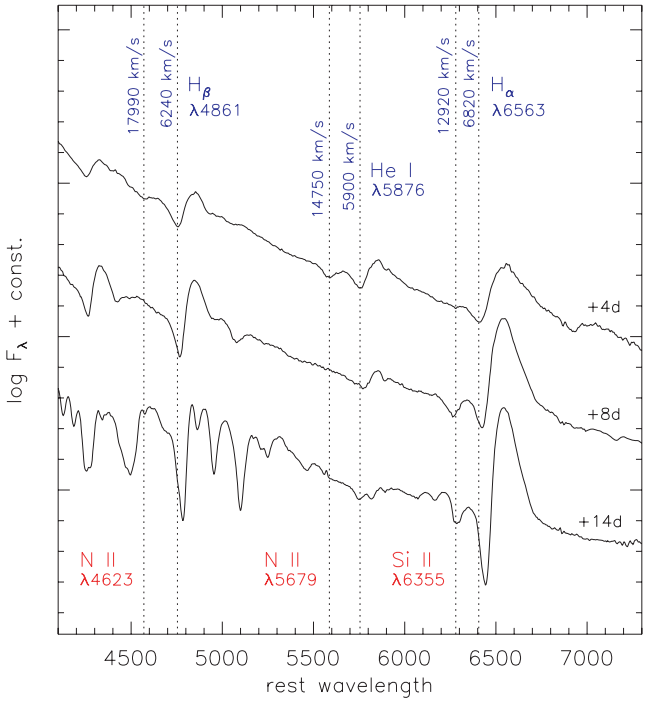

Figure 5. Evolution of the region between 4100 and 7300 Å, where the minima of Hβ, He I 5876 Å and Hα are marked, as well as the position of the features at ∼4580, 5580 and 6300 Å.

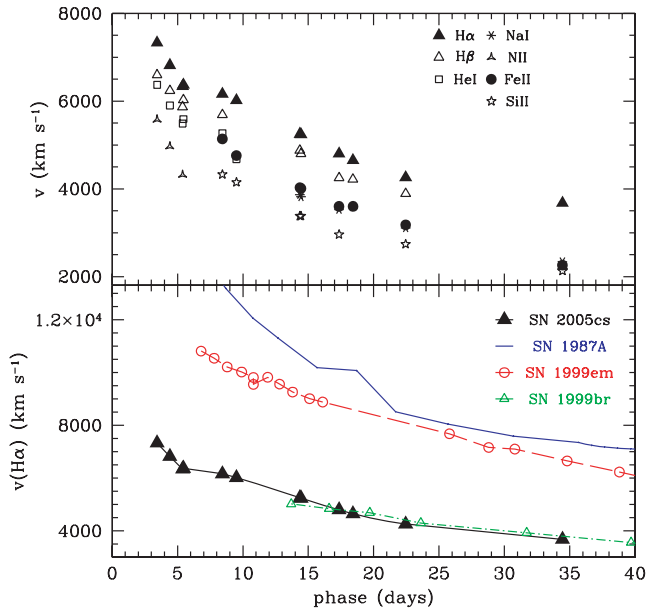

Figure 6. Top panel: expansion velocities for Hα, Hβ, He I λ5876, Na ID, N II λ5680, Fe II λ5169, Si II λ6355 deduced from the minima of P Cygni profiles in the spectra of SN 2005cs. Bottom panel: comparison of the Hα velocity evolution for SN 2005cs, SN 1987A, SN 1999em and SN 1999br. See the text for references.

are marked and the corresponding line velocities are reported. The features at 4580, 5580 and near 6300 Å are also marked, with labelled the two alternative identifications: as putative HV H and He I (with the corresponding line velocities), and as N II and Si II lines (bottom line of Fig. 5). Baron et al. (2000) discuss the identification of the 4580- and 5580-Å features in an early-time spectrum of SN 1999em. Using the simple parametrized code SYNOW (Fisher 2000), in which the relative line strengths for each ion are fixed assuming local thermodynamic equilibrium (LTE), Baron et al. (2000) find that these features could be consistent with N II λ4623 and λ5679. However, the non-LTE model atmosphere code PHOENIX provides a synthetic spectrum which leads them to reject this identification, because it would require an overabundance of nitrogen to reproduce these features. Therefore, they support the identification of the 4580- and 5580-Å absorptions as secondary features of Hβ and He I 5876 Å at high velocity (∼20 000 km s^{-1}), produced by complicated and unexplained non-LTE effects. Alternatively, using the model atmosphere code CMFGEN (Hillier & Miller 1998) and assuming a relevant N enrichment, Dessart & Hillier (2005, 2006) reproduce the lines in the blue wings of both of Hβ and He I 5876 Å detected in the spectra of SN 1999em as N II.

For SN 2005cs, a scenario where two line-forming regions exist for hydrogen and helium is not supported by the line velocities measured for the putative HV components. As shown in Fig. 5, these line velocities are inconsistent. In particular, the velocity of the putative HV Hβ component is much larger than that of the HV Hα component. Moreover, the putative HV Hβ and HV He I features disappear simultaneously in the spectrum at ∼8 d. This supports, at least in the case of SN 2005cs, the identification of these two features as both due to N II.

For the same reason, and because of its persistence over a much longer time than the feature at 4580 Å, we believe that the feature near 6300 Å is Si II 6355 Å, rather than HV Hα. The presence of this absorption in the spectra of SN 1999em was claimed by Dessart & Hillier (2005), and not explicitly mentioned by Baron et al. (2000).

In Fig. 6 (top panel), we show the evolution of the velocity of various absorption spectral lines in SN 2005cs, as derived from the position of their minima. Hα shows the highest velocities, about 1000 km s^{-1} larger than those of the He I line. The N II and the Si II features appear to have smaller velocities than other lines. In particular, the velocity of the N II lines decreases from about 5600 to ∼3200 km s^{-1} between ∼3 and 5 d. The velocity of the Si II 6355-Å feature decreases from 4300 km s^{-1} at ∼8 d to about 2100 km s^{-1} one month after the explosion. Over the same time interval, the Hα velocity decreases from 6200 to 3700 km s^{-1}, while the Fe II velocity is ∼800 km s^{-1} faster than that of the Si II line. In Fig. 6 (bottom panel), we compare the Hα velocity evolution in SN 2005cs with that of SN 1987A (Phillips et al. 1988), SN 1999em (Pastorello 2003) and SN 1999br (Hamuy 2001; Pastorello et al. 2004). The Hα velocity curve of SN 2005cs appears to be strikingly similar to that of the low-velocity SN 1999br.

3.3 Spectral models: the 17- and 34-d spectra

Some preliminary spectral models have been computed in order to provide basic line identification. The code used for the synthetic spectra was described in more detail by Abbott & Lucy (1985), Mazzali & Lucy (1993), Lucy (1999) and Mazzali (2000). The procedure involves a Monte Carlo (MC) simulation of the line transfer based on the Sobolev approximation. The code assumes that all radiative energy is emitted below a sharp lower boundary. The propagation of all energy packets is followed through the spherically symmetric envelope. Processes of interaction for photons taken into account are electron scattering and line transitions. When a photon packet is absorbed by a line transition, it is reemitted at a new frequency corresponding to the branching probabilities for the radiative decays of the excited level. At the end of the MC calculation,

Table 3. Model parameters for synthetic spectra shown in Fig. 7.

	$t = 17$ d	$t = 34$ d
$\log(L/L_\odot)$	7.90	7.88
v_{ph} (km s^{-1})	3710	2580
$\log(R_{ph}/R_\odot)$	3.894	4.037
T_{ph} (K)	7599	6223

a formal integral routine derives the emergent spectrum based on the MC estimate of the source functions (see Lucy 1999).

All models were computed assuming solar composition (Grevesse & Sauval 1998). As a starting point for this preliminary analysis, we used the density structure of the hydrodynamic explosion model adopted to fit SN 1997D (Turatto et al. 1998). This model was characterized by an outer density profile which can be approximated by a power law $\rho \propto r^{-10}$ at velocities above 3000 km s^{-1}, and contained less than $\sim$0.1 $M_\odot$ of material above this velocity. However, in order to reproduce the relatively narrow absorptions, in particular the well separated lines of the Ca II IR triplet, the density structure was cut above $v = 6500$ km s^{-1} by adopting an even steeper power law ($\rho \sim r^{-40}$) beyond that velocity. This modification leads to an insignificant reduction of the ejected mass. Table 3 gives an overview on the model parameters used to derive the synthetic spectra shown in Fig. 7. Input parameters include the total luminosity of the SN and the position of the photosphere in velocity space v_{ph}. Together with the epoch t this constrains the photospheric radius R and, therefore, the temperature at the photosphere via $T_{ph}^4 = L/4\pi\sigma R^2 = L/4\pi\sigma t^2 v_{ph}^2$, where σ is the Stefan–Boltzmann constant. Table 3 gives the final temperature at the photosphere which is determined iteratively to obtain the required emergent luminosity at the outer radius.

The synthetic spectra in Fig. 7 are compared with the observed spectra at phases $\sim$17 (top panel) and 34 d (bottom panel), respectively. The bottom panel of Fig. 7 also shows the identifications of prominent line features in this spectrum. The synthetic spectra support the identification of the feature near 6300 Å with the Si II 6347- and 6371-Å lines. In the region between 5000 and 6400 Å, together with strong Fe II features, prominent lines of Sc II, Ti II and the Na ID lines are identified.

In the later spectrum, we note the increased strength of the Ba II lines compared to earlier epochs. Unfortunately, the 5854-Å line is blended with Na ID and the 6497-Å line with Hα. However, the feature at 6142 Å is relatively unblended and is detected unambiguously. The Ba II lines, as well as those of other s-process elements (Sc and Sr), are particularly prominent in late-photospheric spectra of low-velocity SNe IIP (Pastorello et al. 2004) and SN 1987A, while weaker in other SNe IIP (Mazzali et al. 1992; Mazzali & Chugai 1995; Utrobin & Chugai 2005).

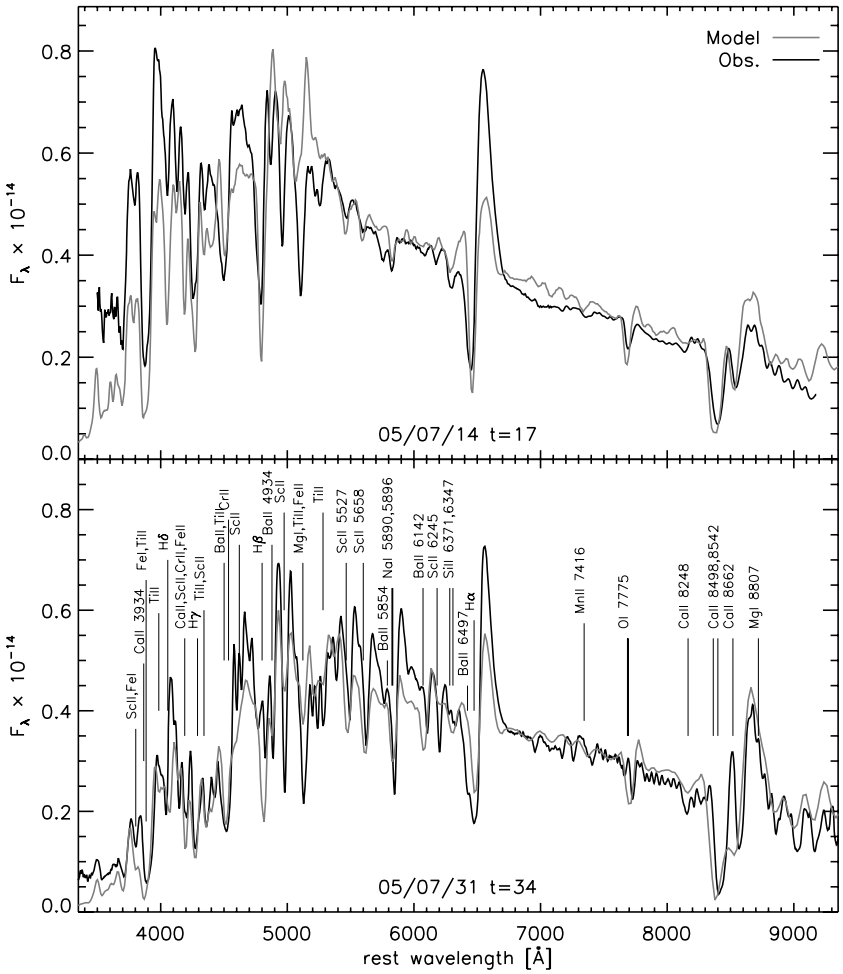

Figure 7. Comparison between synthetic spectra and the observed spectra of SN 2005cs at phase 17 (top panel) and 34 d (bottom panel). The parameters used to compute the synthetic spectra are reported in Table 3.

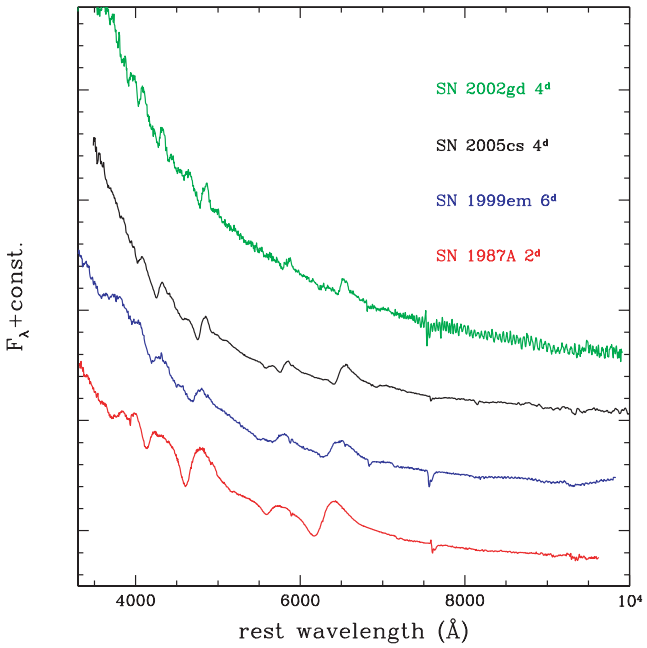

Figure 8. Comparison among spectra of SN 2002gd, SN 2005cs, SN 1999em and SN 1987A shortly after explosion. For references, see the text.

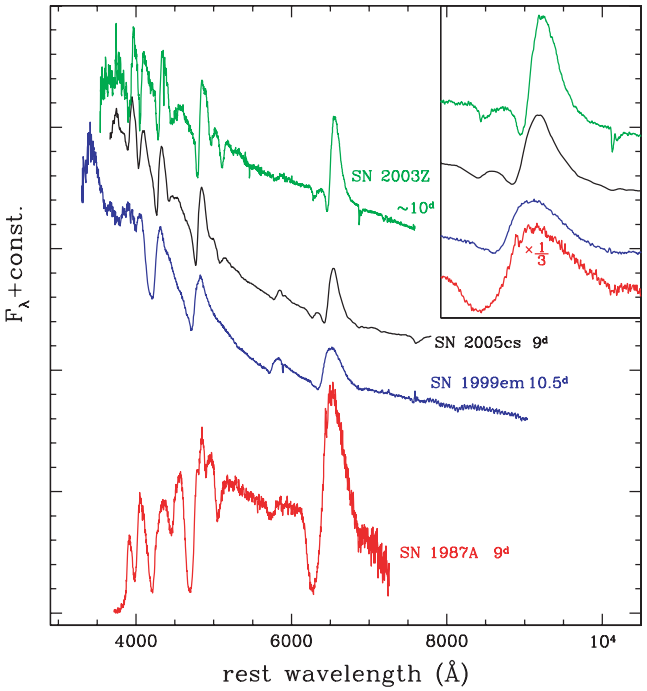

Figure 9. Comparison among spectra of SN 2003Z, SN 2005cs, SN 1999em and SN 1987A at a phase of ∼10 d. A blow-up of the Hα region is shown in the top right-hand side corner, showing the different strengths of the Si II feature in SN IIP spectra.

The proposed density structure does not seem to be able to fit the observations in detail. In particular, it is apparent that the proposed density cut, which is required to fit the Ca II IR lines at $t = 17$ d, does not provide a good fit for the epoch $t = 34$ d. This suggests that a steeper density law with less mass at high velocity is required to reproduce the low-velocity narrow absorptions seen in the observed spectra.

Concerning the total ejected mass, no conclusion can be drawn on the basis of spectral models of early epochs alone. A more detailed analysis of the density structure would also require information on the later spectral evolution as well as a study of the light curve, including the duration of the plateau phase (e.g. Turatto et al. 1998). This will be discussed elsewhere.

3.4 Comparison with other SN IIP

In Fig. 8, we compare the spectrum of SN 2005cs at ∼4 d with those of other young SNe IIP: the low-velocity, ^{56}Ni-poor SN 2002gd (Pastorello 2003), SN 1999em (Hamuy et al. 2001) and SN 1987A (Padova–Asiago SN archive). All spectra have blue continua and show He I 5876 Å and the H Balmer lines. Moreover, the features we attribute to N II 4623 and 5679 Å seem common to all SN II spectra except SN 1987A, which has however broader lines.

At ∼10 d after explosion (see Fig. 9), we note a number of significant differences between the spectra of SNe IIP. While the spectrum of SN 1987A shows a red continuum dominated by prominent H and Fe II P Cygni features, the spectra of more typical SNe IIP are still relatively blue. Although the spectrum of SN 2005cs is slightly redder than that of SN 1999em (Elmhamdi et al. 2003), it is bluer than that of the low velocity and ^{56}Ni-poor SN 2003Z (Knop et al., in preparation). The N II features visible in Fig. 8 have now completely disappeared, but the prominent absorption feature at 6300 Å is now visible in the spectra of SNe 2003Z, 2005cs and, as a bump in the Hα absorption profile, 1999em (see discussion in Elmhamdi et al. 2003). The identification of this feature as Si II 6355 Å is supported by the spectral modelling presented in Section 3.3.

In Fig. 10, we compare the spectrum of SN 2005cs at phase ∼2 weeks to those of the ^{56}Ni-poor SNe 1999br (Hamuy 2001; Pastorello et al. 2004) and 2003Z (Knop et al., in preparation) at a similar epoch. We also include two spectra of SN 1999em (Hamuy et al. 2001; Leonard et al. 2002), taken about 17 and 21 d after the explosion. The Si II 6355-Å feature is prominent in all spectra, included that of SN 1999em at phase ∼17 d, but it is not longer visible 4 d later.

4 DISCUSSION

The observational analogies between SN 2005cs and objects similar to SN 1997D (Turatto et al. 1998) are remarkable. In Table 4, we report some significant information available in the literature for a number of objects belong to this group. Only SNe with very low ejecta velocities and/or small ejected ^{56}Ni mass ($\leqslant 10^{-2}$ M$_\odot$) are included in Table 4. All these objects belong to the faint tail of the luminosity distribution of SNe IIP (Hamuy 2001, 2003; Pastorello 2003; Pastorello et al. 2005; Zampieri 2005) and have similarly low expansion velocities. In particular, the good match between the Hα velocity curves of SNe 2005cs and 1999br (Fig. 6, bottom panel) provides further support to our idea that SN 2005cs can be regarded as another SN 1997D-like event. In analogy to other low-luminosity SNe IIP (Pastorello et al., in preparation), we therefore expect that SN 2005cs will also evolve through a long plateau (3–4 months) and reach a faint late-time luminosity. This would be indicative that a very small mass of ^{56}Ni (of the order of $\sim 10^{-2}$ M$_\odot$ or less) was ejected in the explosion, as the other similar SNe of Table 4.

The earliest spectra of SN 2005cs are very blue, suggesting a very high continuum temperature ($2–3 \times 10^4$ K). In Fig. 11, the evolution

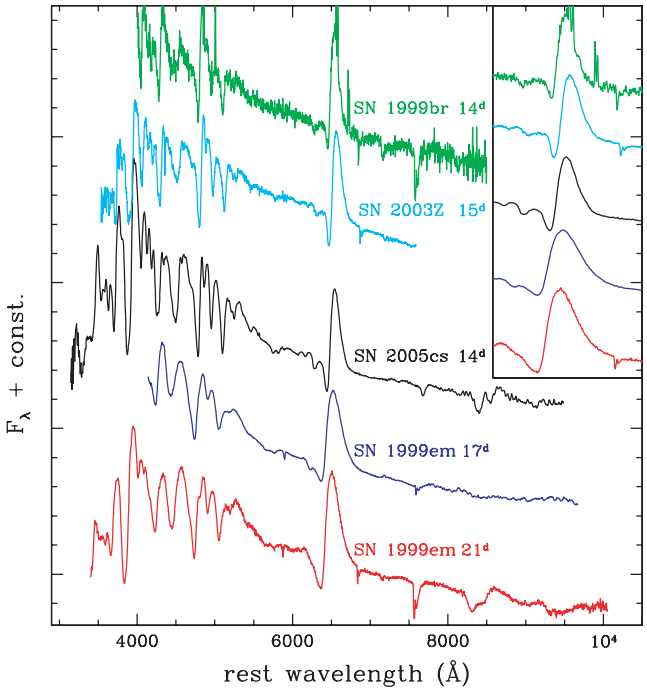

Figure 10. Spectra of the low-velocity SN IIP 1999br, 2003Z and 2005cs at a phase of about two weeks. Spectra of SN 1999em at a phase of 17 and 21 d are included for comparison. Again, a blow-up of the Hα region is also shown in the top right-hand side corner.

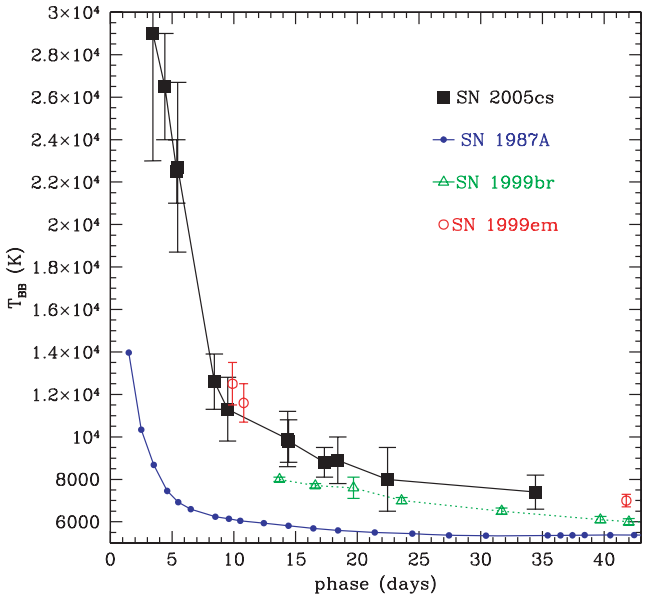

Figure 11. Evolution of the continuum temperature of SNe 2005cs, 1987A, 1999em and 1999br. For references, see the text.

of the temperature of SN 2005cs derived from a blackbody fit to the spectral continuum is compared with those of SN 1987A (Phillips et al. 1988), SN 1999em (as measured in Pastorello 2003) and SN 1999br (Pastorello et al. 2004). Again, the continuum temperature evolution of SN 2005cs is not different from that of other SNe IIP. In particular, SN 2005cs has higher continuum temperatures than SN 1999br, but slightly lower than SN 1999em. Independent of the phase, all these long-plateau SNe have significantly higher continuum temperatures than SN 1987A. The temperature of SN 1987A becomes stationary about three weeks after the explosion, while for other SNe IIP the same happens 30–40 d past explosion. This indicates that in SN 2005cs (and in the other SNe IIP) the H envelope starts to recombine later than in SN 1987A.

If the faint absolute luminosity and the very well developed plateau should be confirmed by the observational campaign still in progress, they would fit with some difficulty the relatively small mass ($M_{\rm ZAMS} \sim 9\,{\rm M}_{\odot}$) progenitor scenario derived from the progenitor detection (Maund et al. 2005; Li et al. 2006). As mentioned in Section 1, both groups argued that the low luminosity of the progenitor indicates that it had a small mass. Maund et al. (2005) obtained a likely range of bolometric luminosity $4 \lesssim \log(L/{\rm L}_{\odot}) \lesssim 4.4$ (shaded region of their fig. 3), and even for conservative errors, $\log(L/{\rm L}_{\odot}) \lesssim 4.6$. Li et al. (2006) obtained an even lower value. To compare with the observed luminosity, they used the Geneva evolutionary models. The highest luminosities attained in the Geneva models are $\log(L/{\rm L}_{\odot}) = 4.2$, 4.5 and 4.8 for $M = 7$, 9 and 12 ${\rm M}_{\odot}$,

Table 4. Main data about low-luminosity and ^{56}Ni-poor SNe IIP available in the literature. In Column 5, we report the expansion velocity of the ejecta at phase ~35 d, obtained from the position of the Hα P Cygni absorption.

SN name	Host galaxy	Galaxy type[a]	$M_{V,{\rm pl}}$[b]	$v_{35}^{H\alpha}$ (km s^{-1})	^{56}Ni mass (M$_{\odot}$)[b]	Source[c]
1994N	UGC 5695	Sab	−14.8	4250	5×10^{-3}	♦
1997D	NGC 1536	SBc	−14.3[d]	–	7×10^{-3}	♦
1999br	NGC 4900	SBc	−13.5	3700	2×10^{-3}	♦
1999eu	NGC 1097	sBb	−13.7[d]	–	$\leqslant 3 \times 10^{-3}$	♦
2000em	LEDA 143614	?	−16.3[e]	–	Unknown	⋆
2001dc	NGC 5777	Sb	−14.1	–	5×10^{-3}	♦
2002gd	NGC 7537	Sbc	−15.6	4100	$\leqslant 3 \times 10^{-3}$	■
2003Z	NGC 2742	Sc	−14.6	4000	5×10^{-3}	■
2004cm	NGC 5486	Sm	−13.9[e]	–	Unknown	*
2004eg	UGC 3053	Sc	−14.7:[e]	–	Unknown	▲
2005cs	M 51	Sbc	−15.2	3700	Unknown	▼

[a] LEDA.
[b] μ computed assuming $H_0 = 72$ km s^{-1} Mpc^{-1}; when possible, $M_{V,{\rm pl}}$ was computed about 1 month after the explosion.
[c] ♦Pastorello et al. (2004); ⋆Strolger et al. (2000); ■Pastorello (2003); ▲Young, Boles & Li (2004); Filippenko et al. (2004); ▼this paper.
*http://cheops1.uchicago.edu/pub/snefchart/sneCand-53088-1324-491-run003712-20-5-0189-00031.html; see also Connolly (2004).
[d] Absolute magnitude measured at the end of plateau.
[e] Unknown phase (but during plateau); *R*-band absolute magnitudes.

respectively. To be consistent with the observed luminosity for the conservative limit, they suggested $M = 7$–$12\,M_{\odot}$ for the progenitor.

However, the Geneva evolutionary models do not reach the pre-supernova stage. They cover the evolution up to the formation of O+Ne+Mg core for $M \geqslant 9\,M_{\odot}$ and only up to the formation of the C+O core for $M = 7\,M_{\odot}$. Stars with $M < 8\,M_{\odot}$ form a degenerate C+O core whose mass $M_{\rm core}$ increases towards the Chandrasekhar mass, $M_{\rm ch}$, as the star climbs the asymptotic giant branch (AGB) (Paczynski 1970). Eventually, the stars will either lose their H-rich envelope to form C+O white dwarfs or undergo a thermonuclear explosion (the so-called Type I 1/2 supernovae) when $M_{\rm core}$ gets close to $M_{\rm ch}$ (for reviews, see Sugimoto & Nomoto 1980; Nomoto & Hashimoto 1988). The 8–10 $M_{\odot}$ stars form a degenerate O+Ne+Mg core whose $M_{\rm core}$ also increases towards $M_{\rm ch}$ on the AGB (Nomoto 1984). Their final fate is also either an O+Ne+Mg white dwarf or a core-collapse supernova when $M_{\rm core}$ gets close to $M_{\rm ch}$ (Nomoto 1984, 1987).

The luminosity L of AGB stars with $M \lesssim 10\,M_{\odot}$ obeys Paczynski's (1970) $M_{\rm core}$–L relation. If a star with $M \lesssim 10\,M_{\odot}$ reaches $M_{\rm core} = 1.4\,M_{\odot}$, the pre-supernova luminosities should be at least $\log(L/L_{\odot}) = 4.8$ for $X({\rm H}) = 0.7$, and even higher if the He abundance is higher (e.g. because of mixing; Hashimoto, Iwamoto & Nomoto 1993). If the progenitor was as massive as $12\,M_{\odot}$, the pre-supernova luminosities would be $\log(L/L_{\odot}) \gtrsim 4.8$. Systematic studies of the progenitor luminosity, including the effect of rotation, would be desirable to obtain a more reliable detailed comparison.

Therefore, the observed luminosity of the putative progenitor of SN 2005cs is inconsistent with the pre-supernova luminosity of 7–$12\,M_{\odot}$ stars. If large extinction causes the observed luminosity of the progenitor to be very small, the observed luminosity cannot be used to constrain the progenitor's mass. One possibility is that the absolute magnitude (and hence the mass) of the progenitor star is underestimated because of dust enshrouding the supergiant progenitor and later swept away by the SN explosion (Graham & Meikle 1986). This scenario was ruled out by Maund et al. (2005) because no K-band excess in the magnitude of the progenitor was detected in archival images. However, we cannot exclude the possibility that a particular dust composition and an extremely low temperature causes the light to be absorbed at optical wavelengths and re-emitted mostly in the mid- and far-IR bands (see e.g. Pozzo et al. 2004). Dust was observed in the late evolution of another well-studied SN IIP, 2003gd (Hendry et al. 2005). Despite having a plateau luminosity and an expansion velocity evolution similar to the 'normal' SN 1999em, SN 2003gd showed low late-time luminosity, indicating the ejection of a small mass of ^{56}Ni (0.015 $M_{\odot}$), only a factor of 2 more than SN 1997D. Van Dyk et al. (2003) and Smartt et al. (2004) found a moderate-mass progenitor for SN 2003gd (8 $M_{\odot}$). However, an evident light echo was recently detected in *HST* images of this object (Sugerman 2005; Van Dyk, Li & Filippenko 2006). This was due to SN light scattered by large-grain dust, located 110–180 pc in front of the SN that survived the initial ultraviolet flash. If this material was present before the SN explosion, it could be responsible for significant extinction of the star light, leading to an underestimate of the luminosity (and hence of the mass) of the progenitor.

As further support to this discussion, most SNe reported in Table 4 exploded in late-type galaxies (mainly of morphological type Sb–Sc, by LEDA,[5]) which would be consistent with massive progenitors.

Finally, there is some ambiguity with regard to the location of the putative progenitor of SN 2005cs. Therefore, even if the works of Maund et al. (2005) and Li et al. (2006) seem to support a moderate mass scenario for the precursor star of SN 2005cs, late-time observations of the explosion site will probably be required in order to remove the residual uncertainty in the correct identification of the progenitor.

[5]http://leda.univ-lyon1.fr/

ACKNOWLEDGMENTS

This work was supported by the Italian Ministry for Education, University and Research (MIUR) under PRIN 2004029938. The observational campaign was coordinated by the Italian Intensive Supernova Program (IISP) (http://web.pd.astro.it/supern/iisp/).

This paper is based on observations collected at the Centro Astronómico Hispano Alemán (Calar Alto, Spain), Asiago and Collurania INAF Observatories (Italy), 1.22-m Galilei Telescope of the Università di Padova (Asiago, Italy), Subaru Telescope (National Astronomical Observatory of Japan, Mauna Kea, USA), Telescopio Nazionale Galileo and Liverpool Telescope (La Palma, Spain).

AP is grateful to M. Turatto, W. Hillebrandt and S. J. Smartt for their useful discussions. We also thank the team of the Osservatorio Astronomico di Cavezzo (Modena, Italy) and M. Barbieri (INAF – Osservatorio Astronomico di Padova) for providing pre-discovery images of the SN 2005cs site. We thank the resident astronomers of Telescopio Nazionale Galileo (in particular Vania Lorenzi), the Liverpool Telescope, and the 2.2- and 3.5-m telescopes in Calar Alto for performing the follow-up observations of SN 2005cs. We also thank Elena Mazzotta Epifani, Roberto Nesci and Giovanna Temporin for the ToO observations of 2005cs at the 1.82-m telescope of Asiago. We are grateful to E. Baron for providing spectra of SN 2003Z before publication and to the SNWeb observers for useful information about very early observations of SN 2005cs.

This research has made use of the NED which is operated by the Jet Propulsion Laboratory, California Institute of Technology, under contract with the National Aeronautics and Space Administration. We also made use of the Lyon-Meudon Extragalactic Database (LEDA), supplied by the LEDA team at the Centre de Recherche Astronomique de Lyon, Observatoire de Lyon.

REFERENCES

Abbott D. C., Lucy L. B., 1985, ApJ, 288, 679
Arnett W. D., Bahcall J. N., Kirshner R. P., Woosley S. E., 1989, ARA&A, 27, 629
Baron E. et al., 2000, ApJ, 545, 444
Benetti S. et al., 2001, MNRAS, 322, 361
Bresolin F., Gamett D. R., Kennicutt R. C., 2004, ApJ, 615, 228
Clocchiatti A., Wheeler J. C., Brotherton M. S., Cochran A. L., Wills D., Barker E. S., Turatto M., 1996, ApJ, 462, 462
Connolly A., 2004, Int. Astron. Union Circ., 8359, 1
Dessart L., Hillier D. J., 2005, A&A, 437, 667
Dessart L., Hillier D. J., 2006, A&A, 447, 691
Elmhamdi A. et al., 2003, MNRAS, 338, 939
Feldmeier J. J., Ciardullo R., Jacoby G. H., 1997, ApJ, 479, 231
Filippenko A. V., Ganeshalingam M., Serduke F. J. D., Hoffman J. L., 2004, Int. Astron. Union Circ., 8404, 1
Filippenko A. V. et al., 1995, ApJ, 450, 11
Fisher A., 2000, PhD thesis, Univ. Oklahoma
Graham J. R., Meikle W. P. S., 1986, MNRAS, 221, 789
Grevesse N., Sauval A. J., 1998, Space Sci. Rev., 85, 161
Hamuy M., 2001, PhD thesis, Univ. Arizona
Hamuy M., 2003, ApJ, 582, 905
Hamuy M. et al., 2001, ApJ, 558, 615
Hashimoto M., Iwamoto K., Nomoto K., 1993, ApJ, 414, L105
Hendry M. A. et al., 2005, MNRAS, 359, 906

Hillier D. J., Miller D. L., 1998, ApJ, 496, 407
Kloehr W., Muendlein R., Li W., Yamaoka H., Itagaki K., 2005, Int. Astron. Union Circ., 8553, 1
Landolt A. U., 1992, AJ, 104, 340
Leonard D. C. et al., 2002, PASP, 114, 35
Leonard D. C., Kanbur S. M., Ngeow C. C., Tanvir N. R., 2003, ApJ, 594, 247
Li W., Van Dyk S. D., Filippenko A. V., Cuillandre J.-C., 2005, PASP, 117, 121
Li W., Van Dyk S. D., Filippenko A. V., Cuillandre J., Jha S., Bloom J. S., Riess A. G., Livio M., 2006, ApJ, 641, L1060
Lucy L. B., 1999, A&A, 345, 211
Maund J., Smartt S. J., 2005, MNRAS, 360, 447
Maund J., Smartt S. J., Danziger I. J., 2005, MNRAS, 364, L33
Mazzali P. A., 2000, A&A, 363, 705
Mazzali P. A., Chugai N. N., 1995, A&A, 303, 118
Mazzali P. A., Lucy L. B., 1993, A&A, 279, 447
Mazzali P. A., Lucy L. B., Butler K., 1992, A&A, 258, 399
Menzies J. W. et al., 1987, MNRAS, 227, 39
Modjaz M., Kirshner R., Challis P., Hutchins R., 2005, Int. Astron. Union Circ., 8555, 1
Nomoto K., 1984, ApJ, 277, 791
Nomoto K., 1987, ApJ, 322, 206
Nomoto K., Hashimoto M., 1988, Phys. Rep., 163, 13
Paczynski B., 1970, Acta Astron., 20, 47
Pastorello A., 2003, PhD thesis, Univ. Padova
Pastorello A. et al., 2004, MNRAS, 347, 74
Pastorello A., Ramina M., Zampieri L., Navasardyan H., Salvo M., Fiaschi M., 2005, in Marcaide J. M., Weiler K. W., eds, IAU Colloq. Vol. 192, Cosmic Explosions, On the 10th Anniversary of SN1993J. Springer-Verlag, Berlin, p. 195
Patat F., Barbon R., Cappellaro E., Turatto M., 1994, A&A, 282, 731
Phillips M. M., Heathcote S. R., Hamuy M., Navarrete M., 1988, AJ, 95, 1087
Pozzo M., Meikle W. P. S., Fassia A., Geballe T., Lundqvist P., Chugai N. N., Sollerman J., 2004, MNRAS, 352, 457
Richmond M. W., 2005, Int. Astron. Union Circ., 8555, 2
Richmond M. W. et al., 1996, AJ, 111, 327
Schlegel D. J., Finkbeiner D. P., Davis M., 1998, ApJ, 500, 525
Smartt S. J., Maund J. R., Hendry M. A., Tout C. A., Gilmore G. F., Mattila S., Benn C. R., 2004, Sci, 303, 499
Sonneborn G., Altner B., Kirshner R. P., 1987, ApJ, 323, L35
Strolger L.-G., Seguel J. C., Krick J., Block A., Candia P., Smith R. C., Suntzeff N. B., Phillips M. M., 2000, Int. Astron. Union Circ., 7524, 2
Sugerman B. E. K., 2005, ApJ, 632, L17
Sugimoto D., Nomoto K., 1980, Space Sci. Rev., 25, 155
Turatto M. et al., 1998, ApJ, 498, 129
Turatto M., Benetti S., Cappellaro E., 2003, in Hillebrandt W., Leibundgut B., eds, From Twilight to Highlight: The Physics of Supernovae. Springer-Verlag, Berlin, p. 200
Utrobin V. P., Chugai N. N., 2005, A&A, 441, 271
Van Dyk S. D., Li W., Filippenko A. V., 2003, PASP, 115, 1289
Van Dyk S. D., Li W., Filippenko A. V., 2006, PASP, 118, 351
Wheeler J. C., Harkness R. P., Clocchiatti A., Benetti S., Brotherton M. S., Depoy D. L., Elias J., 1994, ApJ, 436, 135
Young J., Boles T., Li W., 2004, Int. Astron. Union Circ., 8401, 2
Zampieri L., 2005, in Turatto M., Shea W., Benetti S., Zampieri L., eds, ASP Conf. Ser. Vol. 342, Supernovae as Cosmological Lighthouses. Astron. Soc. Pac., San Francisco, p. 358
Zampieri L., Pastorello A., Turatto M., Cappellaro E., Benetti S., Altavilla G., Mazzali P., Hamuy M., 2003, MNRAS, 338, 711

This paper has been typeset from a TEX/LATEX file prepared by the author.